

Washington University School of Medicine

**Digital Commons@Becker**

---

Open Access Publications

---

2020

## **Microstructural and mechanical properties of grafts commonly used for cruciate ligament reconstruction**

Ryan M Castile

Matthew J Jenkins

Spencer P Lake

Robert H Brophy

Follow this and additional works at: [https://digitalcommons.wustl.edu/open\\_access\\_pubs](https://digitalcommons.wustl.edu/open_access_pubs)

---

# Microstructural and Mechanical Properties of Grafts Commonly Used for Cruciate Ligament Reconstruction

Ryan M. Castile, BS, Matthew J. Jenkins, BS, Spencer P. Lake, PhD, and Robert H. Brophy, MD

*Investigation performed at Washington University in St. Louis, St. Louis, Missouri*

**Background:** Injuries to the anterior cruciate ligament and posterior cruciate ligament are common, and often are treated with reconstruction. Limited quantitative data are available describing material properties of grafts used for reconstructions such as the bone-patellar tendon-bone (BPTB), hamstring tendon (HS), and quadriceps tendon (QT). The purpose of this study was to quantify and compare microstructural and mechanical properties of BPTB, HS, and QT grafts.

**Methods:** Forty specimens (13 BPTB, 13 HS, and 14 QT grafts) from 24 donors were used. Specimens were subjected to preconditioning, stress relaxation, and ramp to failure. Mechanical parameters were calculated for each sample, and polarization imaging was used to evaluate the direction and strength of collagen fiber alignment during testing.

**Results:** QT had the largest modulus values, and HS had the smallest. BPTB exhibited the least disperse collagen organization, while HS were the least strongly aligned. Microstructural properties showed more strongly aligned collagen with increasing load for all grafts. All tissues showed stress relaxation and subtle microstructural changes during the hold period.

**Conclusions:** The mechanical and microstructural properties differed significantly among BPTB, HS, and QT grafts. QT exhibited the largest moduli and greatest strength of collagen alignment, while HS had the smallest moduli and least strongly aligned collagen.

**Clinical Relevance:** This study identified mechanical and microstructural differences among common grafts and between these grafts and the cruciate ligaments they replace. Further research is needed to properly interpret the clinical relevance of these differences.

Injuries to the cruciate ligaments of the knee can destabilize the joint and typically require surgical treatment. The anterior cruciate ligament (ACL) is the most commonly injured ligament of the knee, with >130,000 ACL reconstructions performed yearly in the United States alone<sup>1</sup>. The posterior cruciate ligament (PCL) is reconstructed surgically in patients with acute or chronic isolated grade-III PCL injuries with pain or instability for which an adequate course of non-operative treatment has failed, rare grade-I or II injuries that remain symptomatic after prolonged nonoperative treatment, and multiligament injuries such as combined PCL and posterolateral corner injuries<sup>2,3</sup>. The surgical approach to injuries of the cruciate ligaments is typically reconstruction with a graft.

Graft choice is considered one of the most important modifiable risk factors associated with outcomes of ACL re-

construction<sup>4</sup>. Bone-patellar tendon-bone (BPTB) and the hamstring tendon (HS) are the most commonly used grafts for ACL reconstruction<sup>5</sup>, with growing interest in the quadriceps tendon (QT)<sup>6</sup>. There is variable biomechanical and clinical evidence regarding the relative advantages and disadvantages of these graft choices for ACL reconstruction<sup>7-9</sup>, although many consider BPTB to be the “gold standard.”<sup>10</sup> Similar grafts are used for PCL reconstruction, but little data with which to compare them are available<sup>11</sup>.

The mechanical properties of these grafts have been reported previously<sup>12</sup>. Briefly, the HS was shown to exhibit the largest failure load and stiffness values (2 to 3 times greater than those for the native ACL), whereas the BPTB had slightly lower failure load and similar stiffness compared with the ACL. The QT exhibited similar failure load compared with the native ACL

**Disclosure:** The authors indicated that no external funding was received for any aspect of this work. The **Disclosure of Potential Conflicts of Interest** forms are provided with the online version of the article (<http://links.lww.com/JBJS/G62>).

but ~2 times the stiffness. In contrast to mechanical data, the microstructural properties of these graft tissues have not been reported, to our knowledge. Our recent studies used a polarized light technique to simultaneously assess the mechanical and microstructural properties of the ACL<sup>13-15</sup> and PCL<sup>16</sup>. The purpose of the present study was to determine the mechanical and microstructural properties of the BPTB, HS, and QT to test the hypothesis that these graft tissues have significant differences in material properties that may be related to how well they approximate the properties of native cruciate ligaments.

## Materials and Methods

### Tissue Acquisition

Fresh-frozen cadaveric tissues were collected through Restore Life USA and the Washington University School of Medicine. The samples were acquired without identifiable patient information; therefore, this study was considered exempt by our institutional review board. BPTB and HS samples ( $n = 13$  for each) were harvested from a total of 13 donors (4 male and 9 female; mean age [and standard deviation] at the time of death,  $44 \pm 6$  years), while QT samples ( $n = 14$ ) were harvested from 11 donors (6 male and 5 female; mean age,  $52 \pm 11$  years; 3 bilateral samples). A power analyses based on previous studies<sup>13-15</sup> determined that the target sample size to achieve a 0.7 effect size with alpha set at 0.05 and a power of 0.9 was 14.

Because of variations in anatomical locations and orientations, fine dissections were performed differently for each graft type (Fig. 1) and supervised by an orthopaedic surgeon.

Full-thickness BPTB samples were split into 3 sections: medial, central, and lateral. Five-centimeter-long samples were then cut from the central portion of each of the 3 strips. HS samples were cut from 3 (proximal, central, and distal) 40-mm-long sections along the length. A single  $5 \times 1$ -cm full-thickness QT sample was harvested and then split into 3 layers (superficial, middle, and deep) through the thickness. The QT was split in this fashion due to variability in tendon length, shape, and diameter; the most consistent sampling approach was thus based on depth rather than proximal-distal or medial-lateral referencing.

All harvested samples were prepared for testing using established protocols<sup>13-16</sup>. Briefly, samples were frozen on a freezing-stage (Physitemp Instruments) sledge microtome (Leica) and thinned to  $\sim 600 \mu\text{m}$  to allow for light transmission for polarization imaging. The cross-sectional area was measured using a non-contact laser scanning system (Keyence) in order to convert force values to stress. Samples were then glued between sandpaper tabs (Fig. 1), and 4 beads (0.8 mm in diameter) were glued to the surface to define a central region of interest for microstructural analysis and enable optical strain tracking.

### Testing and Imaging

Graft samples were tested according to protocols used in previous studies of the ACL and PCL<sup>13-16</sup>. Briefly, samples were loaded into a tensile testing machine (TestResources) and submerged in a tissue bath. A quantitative polarized light imaging (QPLI) system, including a division-of-focal-plane polarization camera, was integrated with the mechanical testing machine and

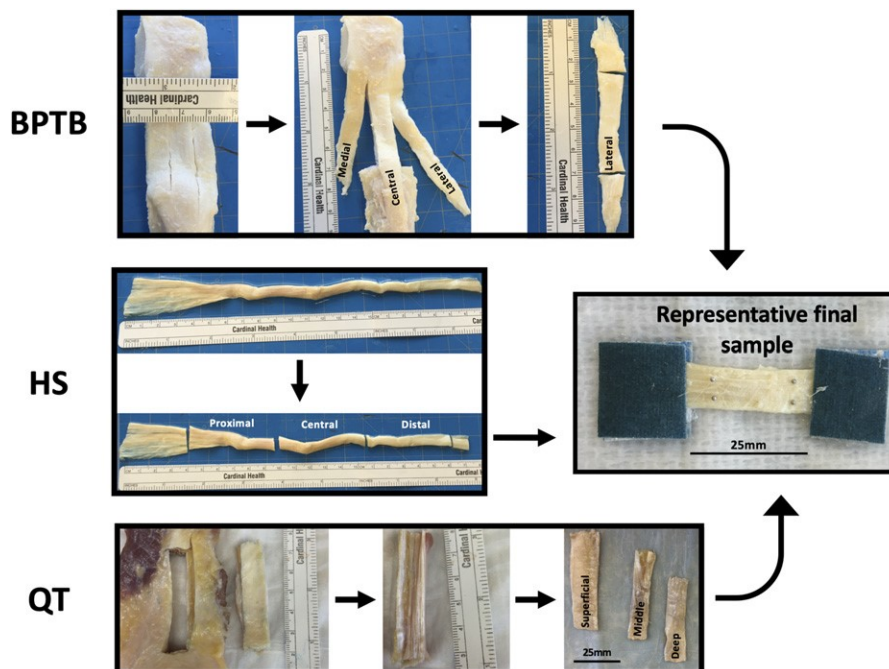


Fig. 1  
BPTB samples were split into medial, central, and lateral thirds; HS samples were split into proximal, central, and distal thirds; and QT samples were separated into superficial, middle, and deep layers. All graft types were trimmed to a length of approximately 40 mm and sandpaper tabs were glued to both ends, allowing for an approximately 25-mm-long region of interest.

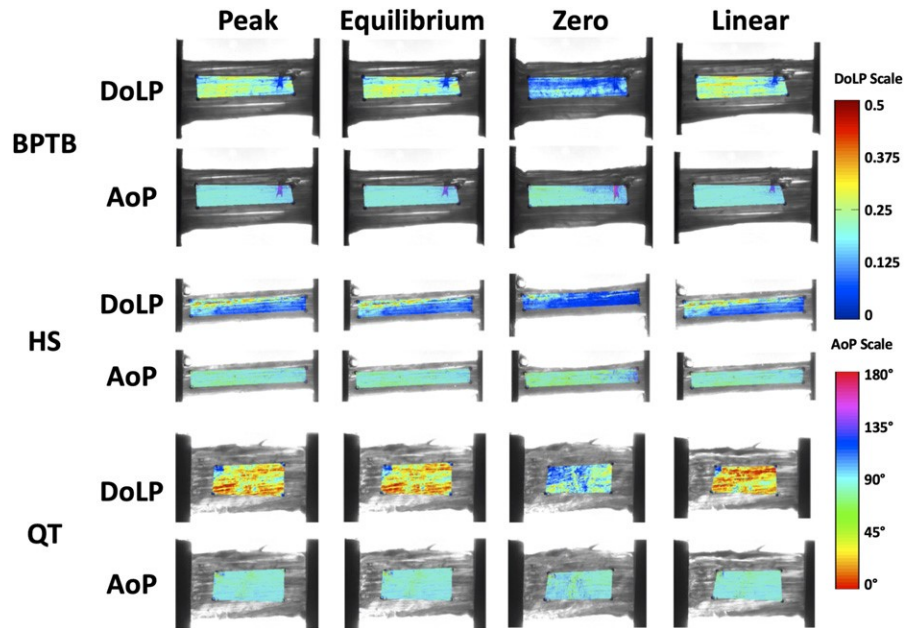


Fig. 2 Representative microstructural heat maps for BPTB, HS, and QT samples. Qualitatively, there were very slight noticeable changes between the peak and equilibrium points for DoLP and AoP in the BPTB, HS, and QT samples. In contrast, all 3 graft types showed an increase in the DoLP (i.e., more reds and yellows in the region of interest) and more uniform collagen alignment (i.e., more of a solid blue AoP map) from the zero to linear points of the ramp-to-failure test.

used to quantify dynamic changes in microstructural properties<sup>13-16</sup>. Samples were preloaded (0.1 N), preconditioned with 10 cycles (1.5% to 4.5% strain at 0.5 Hz), ramped to 5% strain and held for 300 seconds, and then ramped to failure at a rate of 1%/second. Simultaneously, images were acquired at ~19 frames/second and used for optical strain and QPLI analysis.

**Data Analysis**

Surface beads were optically tracked to calculate 2-dimensional strains and extract the strain along the axis of loading. Peak and equilibrium stresses were calculated as the maximum value immediately following the ramp and the steady-state value at the end of the relaxation period, respectively, while percent change was the relative change in stress that occurred during the stress-relaxation test. A bilinear curve fit was applied to the stress-strain data to quantify the elastic modulus in the toe and linear regions and define the transition point between toe and linear regions. Toe modulus provides a measure of relative elasticity in the early loading portion (i.e., at low strain), while linear modulus represents the response at higher strains.

Images corresponding to distinct points during the stress-relaxation (i.e., peak and equilibrium) and quasistatic ramp-to-failure (i.e., zero-, transition-, and linear-strain) phases were used for microstructural analysis (Fig. 2). For each image selected, the average degree of linear polarization (AVG DoLP) and the standard deviation of the angle of polarization (STD AoP) were calculated across the region of interest defined by the 4 surface beads. STD AoP describes the relative uniformity of collagen fiber alignment, while AVG DoLP describes the strength of alignment in a given direction. These parameters provide a quantitative descrip-

tion of the microstructural organization and how that alignment changes during loading.

Nonparametric analyses were employed, and data are presented as median values with interquartile ranges (IQRs). Kruskal-Wallis tests were used to evaluate differences between the sections within a given graft type. With minimal differences detected among the sections of each graft, the values for the subsections were combined and Kruskal-Wallis tests with a Dunn correction for multiple comparisons were used to detect

TABLE I Toe and Linear Moduli for All Regions Taken from Each Sample Type		
	Median Modulus (25%-75% Quartile) (MPa)	
	Toe	Linear
BPTB		
Medial	5.4 (1.3-7.6)	76.9 (55.6-163.1)
Central	4.6 (2.1-10.3)	105.1 (94.3-199.2)
Lateral	4.7 (1.8-7.6)	94.2 (61.6-179)
HS		
Proximal	2.6 (1.5-7.9)	59.1 (44.1-128.6)
Central	2.5 (0.7-3.5)	76.6 (54.2-107.2)
Distal	3.1 (1.9-5.0)	47.6 (34.6-64.8)
QT		
Superficial	12.1 (6.4-23.7)	163.5 (115.2-303.5)
Middle	17.6 (12.6-25.1)	129.5 (105.5-135.2)
Deep	12.5 (4.7-23.6)	176.2 (92.7-310.7)

TABLE II STD AoP at Zero, Transition, and Linear Points for All Regions Taken from Each Sample Type

		Median STD AoP (25%-75% Quartile) (deg)		
		Zero	Transition	Linear
BPTB				
	Medial	8.9 (8.1-12.0)	7.9 (6.2-9.9)	7.4 (5.4-8.7)
	Central	11.4 (9.6-13.2)	8.8 (7.6-10.6)	8.3 (6.8-10.2)
	Lateral	11.8 (11.6-13.6)	9.8 (7.3-11.7)	9.2 (6.9-11.4)
HS				
	Proximal	11.6 (9.8-15.0)	9.2 (8.4-12.6)	8.8 (8.0-11.5)
	Central	14.9 (9.9-15.4)	12.3 (11.4-12.8)	12.3 (11.5-13.2)
	Distal	11.0 (9.9-13.2)	9.1 (8.8-11.9)	8.9 (8.6-11.9)
QT				
	Superficial	11.6 (7.7-20.4)	9.7 (6.5-19.0)	9.3 (6.3-17.9)
	Middle	14.9 (11.5-20.7)	14.2 (10.6-19.0)	14.5 (10.1-17.3)
	Deep	11.0 (7.8-13.3)	9.9 (5.2-15.1)	10.3 (5.1-15.9)

differences among the 3 grafts. Differences with a p value of <0.05 were considered significant.

### Results

There were no statistically significant differences among subsections with respect to modulus (Table I) or STD AoP values (Table II) for any graft type. There were no differences in AVG DoLP among the BPTB subsections, and only limited differences in AVG DoLP between 2 of the HS subsections and among the 3 QT subsections (Table III). Given these results, data for subsections were combined within each graft for subsequent analysis.

Toe and linear modulus values varied by graft type, with QT demonstrating the highest magnitudes, followed by BPTB,

and then by HS (Fig. 3). In the toe region (Fig. 3-A), QT samples exhibited significantly larger moduli (15.7 MPa) compared with both BPTB (5.10 MPa;  $p < 0.001$ ) and HS (2.60 MPa;  $p < 0.0001$ ). In the linear region (Fig. 3-B), modulus values were significantly larger for QT (129.8 MPa) compared with BPTB (97.4 MPa;  $p = 0.041$ ) and HS (62.5 MPa;  $p < 0.0001$ ). BPTB moduli were also significantly larger than HS moduli in the linear region ( $p = 0.018$ ).

Quantitative measures of tissue organization during the ramp to failure demonstrated differences by graft type. AVG DoLP values increased (from zero to transition to linear) for each of the graft types, thereby representing more strongly aligned collagen as load increased (Fig. 4-A). QT demonstrated significantly larger AVG DoLP values (zero = 0.208; transition = 0.260;

TABLE III AVG DoLP at Zero, Transition, and Linear Points for All Regions Taken from Each Sample Type

		Median AVG DoLP (25%-75% Quartile)* (deg)		
		Zero	Transition	Linear
BPTB				
	Medial	0.182 (0.149-0.199)	0.227 (0.174-0.272)	0.241 (0.203-0.277)
	Central	0.187 (0.141-0.226)	0.235 (0.202-0.304)	0.254 (0.219-0.294)
	Lateral	0.138 (0.128-0.196)	0.204 (0.174-0.239)	0.216 (0.191-0.248)
HS				
	Proximal	0.159 (0.122-0.219)	0.199 (0.177-0.287) <sup>a</sup>	0.218 (0.190-0.291) <sup>b</sup>
	Central	0.129 (0.108-0.183)	0.182 (0.150-0.221) <sup>a</sup>	0.198 (0.158-0.242) <sup>b</sup>
	Distal	0.182 (0.171-0.213)	0.225 (0.204-0.260)	0.242 (0.227-0.276)
QT				
	Superficial	0.194 (0.155-0.276)	0.290 (0.235-0.325)	0.295 (0.247-0.338) <sup>d</sup>
	Middle	0.168 (0.141-0.241)	0.207 (0.183-0.258) <sup>c</sup>	0.212 (0.203-0.259) <sup>d,e</sup>
	Deep	0.222 (0.204-0.304)	0.338 (0.256-0.381) <sup>c</sup>	0.324 (0.261-0.362) <sup>e</sup>

\*Values that share a superscripted letter were significantly different ( $p < 0.05$ ) in the within-graft subsection comparisons.



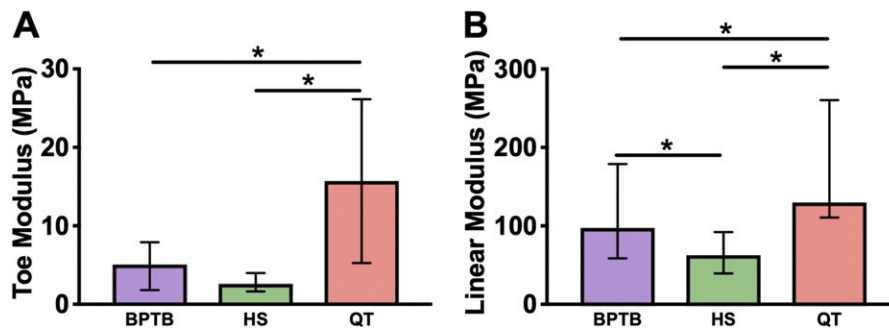


Fig. 3  
**Fig. 3-A** The QT samples had significantly larger toe modulus values compared with both the BPTB and the HS samples, with no difference between BPTB and HS.  
**Fig. 3-B** The QT samples exhibited significantly larger linear modulus values compared with both the BPTB and the HS samples, and the BPTB values were also significantly larger than the HS values. The graphs show the median and IQR. \* $P < 0.05$ .

linear = 0.268) compared with HS at the zero (0.172;  $p = 0.013$ ), transition (0.214;  $p = 0.003$ ), and linear (0.228;  $p = 0.007$ ) points. STD AoP values for BPTB decreased through the ramp, while HS and QT STD AoP values showed small changes during loading (Fig. 4-B). There were no differences by graft type at the zero point for STD AoP values; however, the median BPTB STD AoP value (8.22°) was significantly decreased compared with the HS value (11.5°;  $p = 0.016$ ) and the QT value (11.2°;  $p = 0.008$ ) at the transition point, with similar results at the linear point (7.83° versus 11.1° [ $p = 0.014$ ] and 7.83° versus 11.4° [ $p = 0.008$ ], respectively).

Stress values during the stress-relaxation test were mostly consistent for all grafts (Fig. 5), although QT exhibited significantly larger median value (1.07 MPa) compared with HS at the equilibrium point (0.523 MPa;  $p < 0.0001$ ). During the hold period, stress values for HS decreased significantly more (-43.3%) than both BPTB (-33.5%;  $p < 0.001$ ) and QT (-25.6%;  $p < 0.0001$ ), while BPTB decreased significantly more than QT ( $p < 0.0001$ ). Evaluation of microstructural organization during stress relaxation showed that QT had significantly larger AVG DoLP at peak (0.288) and equilibrium (0.287) compared with BPTB and HS (0.229 [ $p = 0.0036$ ] and 0.220 [ $p < 0.0001$ ], respectively, at peak and

0.236 [ $p = 0.0035$ ] and 0.215 [ $p < 0.0001$ ], respectively, at equilibrium). AVG DoLP values changed only minimally during the hold period, with no significant difference among the graft types. Lastly, STD AoP values were significantly smaller for BPTB at peak (7.86°) and equilibrium (8.10°) compared with both HS and QT (10.9° [ $p = 0.0005$ ] and 10.4° [ $p = 0.0183$ ], respectively, at peak and 11.5° [ $p < 0.0001$ ] and 10.8° [ $p = 0.0081$ ], respectively, at equilibrium). The percent change in the STD AoP was also significantly smaller for BPTB (0.680%) compared with HS and QT (2.58% [ $p = 0.0008$ ] and 2.14% [ $p < 0.0001$ ], respectively). Normalized STD AoP curves showed that BPTB values differed significantly from HS and QT values from approximately 10 seconds onward (Fig. 5-F).

## Discussion

Mechanical and microstructural properties of common cruciate ligament grafts exhibited significant differences by tissue type. QT had the largest modulus values, while the HS moduli were smallest. Consistent with previous data that have shown a relationship between microstructural organization and mechanical properties<sup>13-16</sup>, QT samples were also more strongly aligned compared with HS samples. Interestingly, while

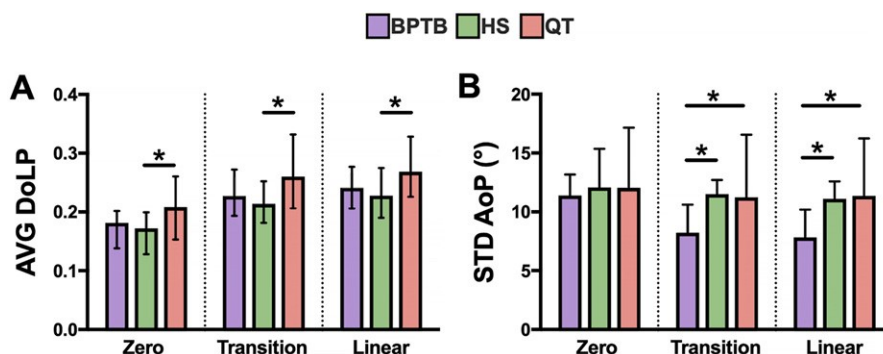


Fig. 4  
**Fig. 4-A** The AVG DoLP values for the HS samples were significantly smaller than those for the QT samples at all points of the ramp. **Fig. 4-B** The STD AoP values at the zero point did not differ by graft type; however, the BPTB values were significantly smaller than both the HS and the QT values at the transition and linear points. The graphs show the median and IQR. \* $P < 0.05$ .

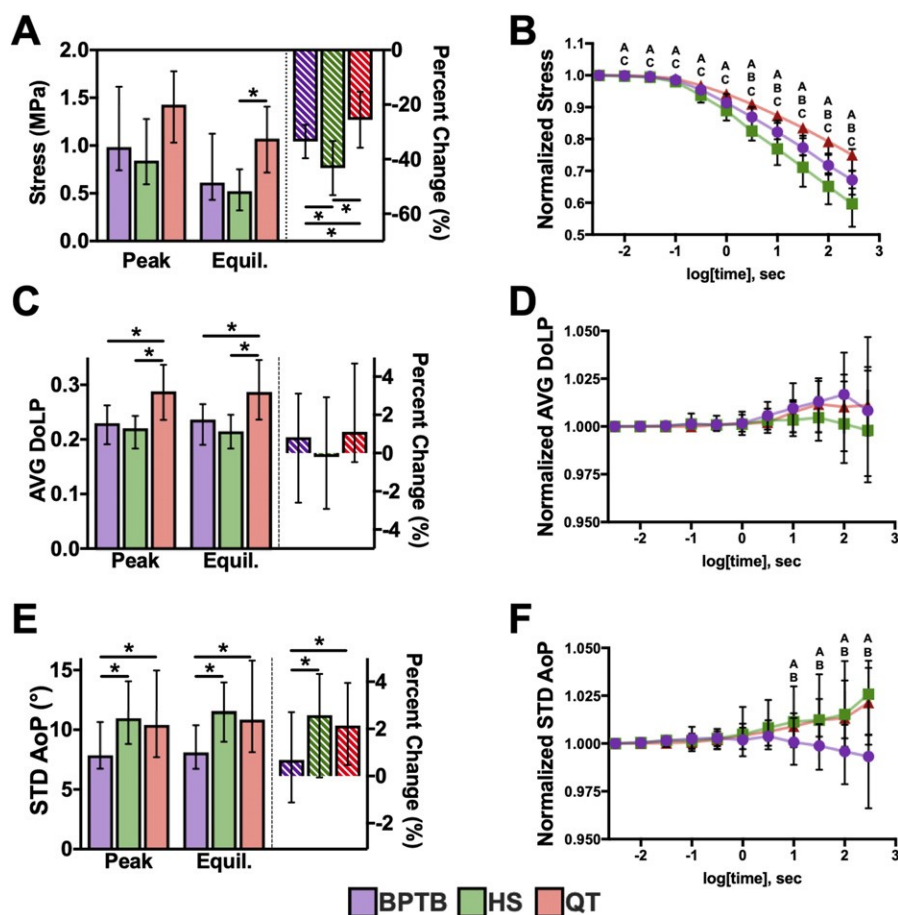


Fig. 5

Median (and IQR) at, and percent change between, peak and equilibrium (Figs. 5-A, 5-C, and 5-E) and time-dependent graphs (Figs. 5-B, 5-D, and 5-F) for stress, AVG DoLP, and STD AoP. In the left graphs, \* indicates  $p < 0.05$ ; in the right graphs, A = significant difference between BPTB and HS, B = significant difference between BPTB and QT, and C = significant difference between HS and QT. Figs. 5-A and 5-B The stress values did not differ by graft type at peak, but HS stress was decreased compared with QT stress at equilibrium (Fig. 5-A). All sample types exhibited significantly different amounts of stress relaxation (i.e., percent change) (Fig. 5-A), which is also evident in the time-dependent graph (Fig. 5-B). Figs. 5-C and 5-D The AVG DoLP values were significantly larger for the QT samples compared with both the BPTB and the HS samples at peak and equilibrium, but there was no differences among graft types over time with regard to percent change (Fig. 5-C) or in the time-dependent curves (Fig. 5-D). Figs. 5-E and 5-F The STD AoP values were significantly smaller in the BPTB samples compared with both HS and QT at peak and equilibrium, and the percent change was also significantly smaller for BPTB compared with HS and QT (Fig. 5-E) and at later times (Fig. 5-F).

no differences in spread of alignment were apparent in the unloaded state, BPTB showed more uniform alignment when loaded compared with both QT and HS.

In previous data sets<sup>13-16</sup>, QPLI parameters usually demonstrated an inverse relationship; greater strength of alignment (i.e., large AVG DoLP) generally corresponded with greater uniformity of alignment (i.e., small STD AoP). In the current data set, this pattern was not evident for the QT samples. Given the large AVG DoLP values for QT, small STD AoP values would have been expected. However, the results can be understood by considering the anatomy of the QT, a composite tissue that forms from the confluence of 4 musculotendinous units<sup>6,11</sup>. The QT has been shown to have significant variability in fiber orientation<sup>17</sup>, which is consistent with our observations during dissections that tendon structures in the intermediate layer of the QT interdigitate from

both the medial and the lateral orientation. Microstructural data for the BPTB and HS followed expected patterns relating quantitative measures of tissue organization to mechanical properties.

In this study of material properties, HS samples exhibited the smallest modulus values, which is in contrast to previous tests at the full tissue level that showed greater stiffness compared with the QT and BPTB<sup>17</sup>. This apparent discrepancy is due to differences in how samples were prepared (i.e., thinned versus full-thickness samples) and which specific parameters were evaluated. Reported structural parameters of stiffness and failure load depend on total graft cross-sectional area. Similarly, the material properties of the QT and BPTB measured in the current study showed some differences compared with the structural parameters measured previously at the tissue level for these grafts; however, the results were more similar for QT and BPTB than for HS samples<sup>18</sup>.

Previous studies quantified the mechanical and microstructural properties of the ACL<sup>13-15</sup> and PCL<sup>16</sup>. While a gradient of changes in properties was seen across regions of the ACL, the graft tissues evaluated in the present study did not demonstrate significant inter-regional variation. Thus, the graft tissues appear to have fairly homogeneous properties throughout their length, width, and thickness (of the HS, BPTB, and QT, respectively), findings that are similar to those for the PCL<sup>16</sup>. Comparing graft material properties to parameters for the ACL and PCL obtained using the same test setup and protocol can provide insights that would be useful when considering suitability of various grafts for cruciate ligament reconstruction. For example, the linear modulus was smaller for the ACL (IQR: 9.9 to 46.3 MPa)<sup>13</sup> and PCL (IQR: 56.2 to 137 MPa)<sup>16</sup> compared with the QT and BPTB, and for the ACL compared with the HS. With regard to unloaded microstructural properties, AVG DoLP values were smaller for the ACL (IQR: 0.124 to 0.193)<sup>13</sup> and PCL (IQR: 0.112 to 0.186)<sup>16</sup> compared with the QT, BPTB, and HS. Lastly, unloaded STD AoP values for the ACL (IQR: 18.9° to 28.4°)<sup>13</sup> and PCL (IQR: 11.8° to 18.2°)<sup>16</sup> were larger than the values for the QT, BPTB, and HS. Overall, there were mechanical and microstructural differences between the grafts and the cruciate ligaments that they reconstruct.

The clinical implications of these findings are speculative as this study does not contain any data on the relationship of these properties, if any, with biologic or clinical outcomes of ligament reconstruction. Matching graft properties to native ligaments at the time of reconstruction could be advantageous. The baseline material properties suggest that hamstrings could have an advantage compared with extensor tendons due to the lower modulus for the ACL; however, the PCL moduli are more similar to the BPTB moduli. The QT may have a slight disadvantage compared with the HS and even the BPTB due to its higher moduli. A higher modulus does not necessarily mean a better graft as there are multiple factors to consider, such as graft size, repair technique, and graft tensioning. A very important confounder is that it is not known how tissue properties change after reconstruction during the process of ligamentization<sup>19,20</sup>. More research is needed to properly interpret the clinical relevance of differences among grafts for ligament reconstruction.

Limitations of this study include an average age of graft donors that is older than the typical age of patients undergoing reconstruction, which has potential implications since autografts are preferred in younger patients<sup>21</sup>. Allografts are more commonly used in older patients and are likely to come from a donor population similar in age to our study cohort<sup>22</sup>. The tissues used for this study were frozen on acquisition. While samples did undergo limited freeze-thaw cycles, this was unlikely to have had any major effect on the tissues<sup>23-28</sup>, particularly since they did not undergo any sterilization process. The QT samples came from a different donor population than the HS and BPTB samples, potentially introducing a confounding bias to the anal-

ysis. Conversely, one could argue that using samples from diverse donors makes the study more generalizable. Additionally, harvested tissues were dissected and thinned to enable analysis with our polarization imaging technique, meaning that anatomical and geometrical conditions were not the same as during cruciate ligament reconstructions; however, this approach was chosen to provide a full quantitative description of material properties. Such a reductionist approach is necessary to assess the microstructural properties of the grafts, but obviously it does not reflect the macrostructure of the grafts as used for ligament reconstruction (i.e., 4-strand HS or full-thickness QT grafts). Mechanical testing of the QT is known to be challenging due to the variability of the location of insertion of various parts of the tendon into the proximal pole of the patella<sup>29</sup>, making it difficult to section on the basis of proximal-distal or medial-lateral referencing. While we attempted to overcome such issues with our dissection protocol, some of the variability in our QT data may be related to anatomical aspects of this complex tendon, including a lack of sampling at the interface between the layers of the QT. As with any cadaver study, there is no information on what medications or supplements the donors were taking and/or what diseases or conditions were ruled out. The hydration status of the donor at the time of death could have been variable as well, although it is unlikely to have substantially altered the microstructural properties of these tissues.

In conclusion, mechanical and microstructural properties of grafts commonly used for cruciate ligament reconstruction have significant differences that suggest a potential advantage of the hamstring compared with the extensor tendons. The precise implications of these differences in material properties for biologic healing and clinical outcomes are yet to be determined. Further study is warranted to see if and how these properties change following surgery and relate to the outcomes of these common surgical procedures. ■

Ryan M. Castile, BS<sup>1</sup>  
Matthew J. Jenkins, BS<sup>1</sup>  
Spencer P. Lake, PhD<sup>1</sup>  
Robert H. Brophy, MD<sup>1</sup>

<sup>1</sup>Departments of Mechanical Engineering & Materials Science (R.M.C., M.J.J., and S.P.L.) and Orthopaedic Surgery (S.P.L. and R.H.B.), Washington University in St. Louis, St. Louis, Missouri

Email address for R.M. Castile: castiler@wustl.edu

ORCID iD for R.M. Castile: [0000-0002-1974-2106](https://orcid.org/0000-0002-1974-2106)  
ORCID iD for M.J. Jenkins: [0000-0003-3623-9577](https://orcid.org/0000-0003-3623-9577)  
ORCID iD for S.P. Lake: [0000-0002-7424-947X](https://orcid.org/0000-0002-7424-947X)  
ORCID iD for R.H. Brophy: [0000-0002-2912-8265](https://orcid.org/0000-0002-2912-8265)

## References

1. Mall NA, Chalmers PN, Moric M, Tanaka MJ, Cole BJ, Bach BR Jr, Paletta GA Jr. Incidence and trends of anterior cruciate ligament reconstruction in the United States. *Am J Sports Med.* 2014 Oct;42(10):2363-70. Epub 2014 Aug 1.

2. Matava MJ, Ellis E, Gruber B. Surgical treatment of posterior cruciate ligament tears: an evolving technique. *J Am Acad Orthop Surg.* 2009 Jul; 17(7):435-46.



3. Montgomery SR, Johnson JS, McAllister DR, Petrigliano FA. Surgical management of PCL injuries: indications, techniques, and outcomes. *Curr Rev Musculoskelet Med*. 2013 Jun;6(2):115-23.
4. Duchman KR, Lynch TS, Spindler KP. Graft selection in anterior cruciate ligament surgery: who gets what and why? *Clin Sports Med*. 2017 Jan;36(1):25-33. Epub 2016 Oct 15.
5. Tibor L, Chan PH, Funahashi TT, Wyatt R, Maletis GB, Inacio MC. Surgical technique trends in primary ACL reconstruction from 2007 to 2014. *J Bone Joint Surg Am*. 2016 Jul 6;98(13):1079-89.
6. Slone HS, Romine SE, Premkumar A, Xerogeanes JW. Quadriceps tendon autograft for anterior cruciate ligament reconstruction: a comprehensive review of current literature and systematic review of clinical results. *Arthroscopy*. 2015 Mar;31(3):541-54. Epub 2014 Dec 25.
7. Offerhaus C, Albers M, Nagai K, Arner JW, Höher J, Musahl V, Fu FH. Individualized anterior cruciate ligament graft matching: in vivo comparison of cross-sectional areas of hamstring, patellar, and quadriceps tendon grafts and ACL insertion area. *Am J Sports Med*. 2018 Sep;46(11):2646-52. Epub 2018 Jul 30.
8. Lansdown DA, Riff AJ, Meadows M, Yanke AB, Bach BR Jr. What factors influence the biomechanical properties of allograft tissue for ACL reconstruction? A systematic review. *Clin Orthop Relat Res*. 2017 Oct;475(10):2412-26.
9. Cerulli G, Placella G, Sebastiani E, Tei MM, Speziali A, Manfreda F. ACL reconstruction: choosing the graft. *Joints*. 2013 Jun 12;1(1):18-24.
10. Höher J, Scheffler S, Weiler A. Graft choice and graft fixation in PCL reconstruction. *Knee Surg Sports Traumatol Arthrosc*. 2003 Sep;11(5):297-306. Epub 2003 Aug 26.
11. Thauinat M, Fayard JM, Sonnery-Cottet B. Hamstring tendons or bone-patellar tendon-bone graft for anterior cruciate ligament reconstruction? *Orthop Traumatol Surg Res*. 2019 Feb;105(1S):S89-94. Epub 2018 Aug 18.
12. Mehran N, Damodar D, Shu Yang J. Quadriceps tendon autograft in anterior cruciate ligament reconstruction. *J Am Acad Ortho Surg*. 2020 Jan 15;28(2):45-52.
13. Skelley NW, Castile RM, York TE, Gruev V, Lake SP, Brophy RH. Differences in the microstructural properties of the anteromedial and posterolateral bundles of the anterior cruciate ligament. *Am J Sports Med*. 2015 Apr;43(4):928-36. Epub 2015 Jan 29.
14. Castile RM, Skelley NW, Babaei B, Brophy RH, Lake SP. Microstructural properties and mechanics vary between bundles of the human anterior cruciate ligament during stress-relaxation. *J Biomech*. 2016 Jan 4;49(1):87-93. Epub 2015 Nov 22.
15. Skelley NW, Castile RM, Cannon PC, Weber CI, Brophy RH, Lake SP. Regional variation in the mechanical and microstructural properties of the human anterior cruciate ligament. *Am J Sports Med*. 2016 Nov;44(11):2892-9. Epub 2016 Jul 25.
16. Wright JO, Skelley NW, Schur RP, Castile RM, Lake SP, Brophy RH. Microstructural and mechanical properties of the posterior cruciate ligament: a comparison of the anterolateral and posteromedial bundles. *J Bone Joint Surg Am*. 2016 Oct 5;98(19):1656-64.
17. Waligora AC, Johanson NA, Hirsch BE. Clinical anatomy of the quadriceps femoris and extensor apparatus of the knee. *Clin Orthop Relat Res*. 2009 Dec;467(12):3297-306. Epub 2009 Aug 19.
18. Shani RH, Umpiarez E, Nasert M, Hiza EA, Xerogeanes J. Biomechanical comparison of quadriceps and patellar tendon grafts in anterior cruciate ligament reconstruction. *Arthroscopy*. 2016 Jan;32(1):71-5. Epub 2015 Sep 14.
19. Amiel D, Kleiner JB, Roux RD, Harwood FL, Akeson WH. The phenomenon of "ligamentization": anterior cruciate ligament reconstruction with autogenous patellar tendon. *J Orthop Res*. 1986;4(2):162-72.
20. Dong S, Xie G, Zhang Y, Shen P, Huangfu X, Zhao J. Ligamentization of autogenous hamstring grafts after anterior cruciate ligament reconstruction: midterm versus long-term results. *Am J Sports Med*. 2015 Aug;43(8):1908-17. Epub 2015 Jun 1.
21. Kaeding CC, Aros B, Pedroza A, Pifel E, Amendola A, Andrish JT, Dunn WR, Marx RG, McCarty EC, Parker RD, Wright RW, Spindler KP. Allograft versus autograft anterior cruciate ligament reconstruction: predictors of failure from a MOON prospective longitudinal cohort. *Sports Health*. 2011 Jan;3(1):73-81.
22. Jost PW, Dy CJ, Robertson CM, Kelly AM. Allograft use in anterior cruciate ligament reconstruction. *HSS J*. 2011 Oct;7(3):251-6. Epub 2011 Aug 19.
23. Jung HJ, Vangipuram G, Fisher MB, Yang G, Hsu S, Bianchi J, Ronholdt C, Woo SL. The effects of multiple freeze-thaw cycles on the biomechanical properties of the human bone-patellar tendon-bone allograft. *J Orthop Res*. 2011 Aug;29(8):1193-8. Epub 2011 Mar 4.
24. Lee AH, Elliott DM. Freezing does not alter multiscale tendon mechanics and damage mechanisms in tension. *Ann N Y Acad Sci*. 2017 Dec;1409(1):85-94. Epub 2017 Oct 25.
25. Huang H, Zhang J, Sun K, Zhang X, Tian S. Effects of repetitive multiple freeze-thaw cycles on the biomechanical properties of human flexor digitorum superficialis and flexor pollicis longus tendons. *Clin Biomech (Bristol, Avon)*. 2011 May;26(4):419-23. Epub 2011 Jan 8.
26. Lee GH, Kumar A, Berkson E, Verma N, Bach BR Jr, Hallab N. A biomechanical analysis of bone-patellar tendon-bone grafts after repeat freeze-thaw cycles in a cyclic loading model. *J Knee Surg*. 2009 Apr;22(2):111-3.
27. Ng BH, Chou SM, Lim BH, Chong A. The changes in the tensile properties of tendons after freeze storage in saline solution. *Proc Inst Mech Eng H*. 2005 Nov;219(6):387-92.
28. Moon DK, Woo SL, Takakura Y, Gabriel MT, Abramowitch SD. The effects of refreezing on the viscoelastic and tensile properties of ligaments. *J Biomech*. 2006;39(6):1153-7. Epub 2005 Apr 5.
29. Stäubli HU, Schatzmann L, Brunner P, Rincón L, Nolte LP. Quadriceps tendon and patellar ligament: cryosectional anatomy and structural properties in young adults. *Knee Surg Sports Traumatol Arthrosc*. 1996;4(2):100-10.